



Urban landscape classification using Chinese advanced high-resolution satellite imagery and an object-oriented multi-variable model^{*}

Li-gang MA^{†1}, Jin-song DENG^{†‡1,2}, Huai YANG¹, Yang HONG^{2,3}, Ke WANG^{†‡1}

⁽¹⁾*Institute of Applied Remote Sensing & Information Technology, Zhejiang University, Hangzhou 310058, China*

⁽²⁾*School of Civil Engineering and Environmental Sciences and School of Meteorology, University of Oklahoma, Norman, OK 73019, USA*

⁽³⁾*State Key Laboratory of Hydrosience and Engineering, Department of Hydraulic Engineering, Tsinghua University, Beijing 100084, China*

[†]E-mail: 11114054@zju.edu.cn; jsong_deng@zju.edu.cn; Kwang@zju.edu.cn

Received Mar. 7, 2014; Revision accepted May 30, 2014; Crosschecked

Abstract: The Chinese ZY-1 '02C' satellite is one of the most advanced high-resolution earth observation systems designed for terrestrial resource monitoring. Its capability for comprehensive landscape classification, especially in urban areas has been under constant study. In view of the limited spectral resolution of the ZY-1 02C satellite (three bands); combined with the complexity and heterogeneity across urban environments, this study attempts to test its capability to classify urban landscape by combing a multi-variable model with an object-oriented approach. The multiple variables including spectral reflection, texture, spatial autocorrelation, impervious surface fraction, vegetation and geometry indexes were first calculated and selected for relevance using the Forward Stepwise Linear Discriminant analysis and then applied in the following object-oriented classification process. Comprehensive accuracy assessment which adopts traditional Error Matrices with stratified random samples and Polygon Area Consistency (PAC) indexes was subsequently conducted to examine the real area agreement between a classified polygon and its references. Results indicated that the overall classification accuracy was 92.63% and the Kappa statistics were 0.9124. Furthermore, the proposed PAC index showed that more than 82% of all polygons were correctly classified. Although there exists some misclassification mostly between residential and barren/farmland, the presented method and the Chinese ZY-1 '02C' satellite imagery were assessed to be robust and effective for urban landscape classification.

Key words: ZY-1 '02C' satellite, Classification, Urban, Multi-variable model

doi:10.1631/jzus.C1400083

Document code: A

CLC number:

1 Introduction

Remote sensing technology is widely applied in various fields and is also one of the most efficient means of studying urban land cover, structure, landscape and the eco-environment. With the fast-pace changes in urban landscapes, particularly in rapidly expanding metropolitan regions, the acquirement of frequently updating land use datasets has become a

routine assignment. Consequently, deriving timely and accurate land-use information so as to keep pace with urban development is a critical challenge confronting urban planners (Hu and Wang, 2013). Requirements of land-use mapping and monitoring by means of automated classification on remote sensing imagery have played an increasingly important role in decision-making and urban management.

In terms of remote sensing technology, earth observing satellites are able to acquire abundant image data, ranging from high resolutions (i.e., 0.5-1 m such as GeoEye, WorldView, IKONOS, and Quick-Bird) to moderate resolutions (i.e., 10-30 m such as SPOT, ALOS, ASTER, and LANDSAT) for mapping urban landscapes. However, an overwhelming majority of satellite images are dominated by the United

[‡] Corresponding author

^{*} Project supported by grants from the national high-tech industrialization application of special projects (No. 2009214), Zhejiang key scientific and technological innovation team projects (No. 2010R50030) and the National Natural Science Foundation of China (No. 31172023)

© Zhejiang University and Springer-Verlag Berlin Heidelberg 2014

States and European space agencies. In recent years, China has launched a series of high-resolution satellites among which ZY-1 02C is one of the most advanced. Although the satellite is only equipped with three spectral bands (Green, Red, NIR) which may increase the difficulty for discriminating urban targets, there is an urgent need to examine its utility and capabilities in detecting subtle changes in urban land use and land cover. More in-depth information about this ZY-1 02C satellite imagery can be found in Table 1.

Additionally, information extraction and classification techniques are other crucial aspects of image analysis. A large number of classification algorithms have been developed during the past decades. In view of image processing concepts, they can be grouped as ‘traditional’ single pixel-based and ‘object-oriented’ classification methods. It is generally stated that object-oriented classification often outperforms the pixel-based method in high-resolution imagery and could extract tangible information which is well-suited to combine with vector GIS data. Chen *et al.* (2007) demonstrated the potential of object based image analysis (OBIA) to map urban land cover for the city of Beijing from ASTER data with a relatively high accuracy. Durieux *et al.* (2008) proposed precise monitoring of building construction using an object-based classification methodology applied to SPOT5 images. Jacquin *et al.* (2008) assessed the ability of an object-based approach in classifying urban objects at multiple spatial scales with SPOT5 images. The images acquired by 02C satellite have similar spatial resolution to SPOT and ASTER; urban mapping with this data through an object oriented approach could probably yield acceptable results. Therefore, we attempt to explore a method, based on the characteristics of this kind of imagery (relatively high spatial resolution and low spectral resolution), which integrates five categories of variables (fraction of impervious surface, vegetation index, texture derived from Gray Level Co-occurrence Matrix, spatial autocorrelation and shape related features) for urban classification with an object-based approach.

Table 1 Basic parameters of the 02C satellite

Parameter	P/MS camera
Wavelength	B1:0.52-0.59 μm (Green)
	B2:0.63-0.69 μm (Red)
	B3:0.77-0.89 μm (NIR)

Spatial Resolution	10 m
Swath	60 Km
Side-sway ability	$\pm 32^\circ$
Revisiting period	3-5 d
Coverage period	55 d
Phase	2012-2-28

2 Methods

2.1 Study Area

The study area is Hangzhou city, the capital of Zhejiang Province which lies in the southern wing of the Yangtze Delta (Fig. 1) covering an area of 3068 km² (720 km² for the city proper) with a population of 3.932 million (Deng *et al.*, 2008). This city experienced a rapid expansion during the past decade while its historical and modern buildings coexist due to heritage policy on historical and cultural protection. Since 1978, industrial zones and commercial buildings sprang up extensively across Hangzhou city after China’s economic reform. The diversity of land-cover makes it an extremely challenging task for classification, thus it represents an ideal place for urban classification study.

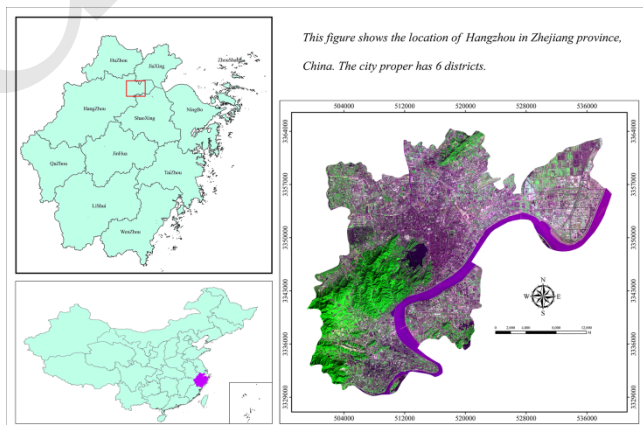


Fig. 1 Geographic location of Hangzhou City, Zhejiang Province, China

2.2 Data sets used in current research

A multispectral image with 10 meter spatial resolution acquired in February, 2012 by the P/MS sensor of the ‘02C’ satellite is examined in this study. A fine land-use map derived from a visually interpreted high-resolution aerial photo in 2010 was used

as the reference data. Field survey data, including GPS positions and photos acquired in 2012, were adopted as additional reference data for an assessment of the land use classification accuracy.

2.3 Image Processing

Using the referencing on the high resolution image and the in-field GPS survey, geometric cor-

rection was first conducted. Altogether, thirty GCP (ground control points) were selected and 0.5 RMSE was achieved to guarantee geometric fidelity.

As shown in Fig. 2, our classification scheme is composed of 5 steps: (1) Variable calculation; (2) Feature selection; (3) Correlation and variable importance analysis; (4) Object oriented classification; (5) Accuracy assessment.

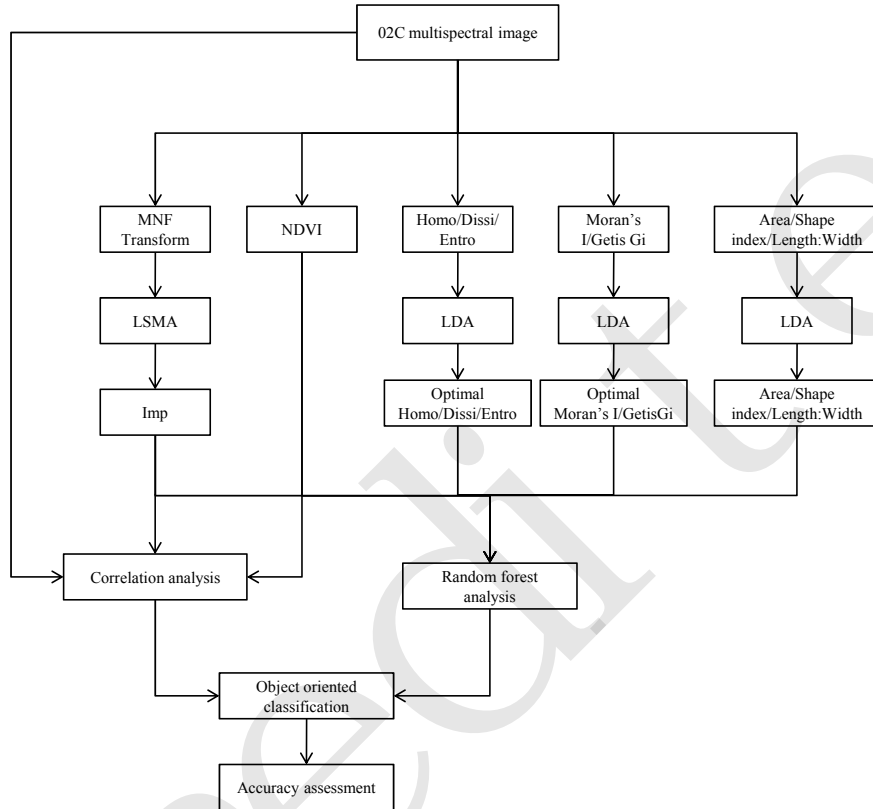


Fig. 2 Flow chart of the proposed method consisting of impervious surface(Imp) extraction, Homogeneity/ Dissimilarity/Entropy (Homo/Dissi/Entro) and Moran's I/Getis-Ord Gi calculation, linear discriminant analysis (LDA), etc.

2.4 Variable calculation and selection

(1) Fraction Images

Ridd (1995) pointed out that urban areas can be divided into three parts, namely impervious surfaces, vegetation and soil. Theoretically, the percentage of impervious surface may contribute to the improvement of urban image classification since this feature should be different for different land-use types. In practice, linear spectral mixture analysis (LSMA) has shown the potential for estimating impervious surfaces and improving urban classification (Lu and Weng, 2006).

Mixed pixel problems, as well as extraction of quantitative sub-pixel information in satellite imagery with medium or coarse spatial resolution, are usually solved by means of applying the SMA technique (Smith *et al.*, 1990). It has been hypothesized, that a linear combination of the spectra of all components within a pixel, constitute the spectrum measured by a sensor (Adams *et al.*, 1995). The principle and detailed description can be found in Settle and Drake (1993). In this research, a minimum noise transform (MNF) was applied to the image, and three end-members: impervious surface, vegetation and shade were then selected from the feature space of the MNF

components. Residential area was identified for the impervious surface end member selection, while vegetation was selected from trees and dense grass. The shade end-member was selected from rivers and lakes. The original three multispectral images were unmixed into three fraction images with a least square solution. Impervious surface fractions were finally extracted.

(2) Vegetation Indices

Researchers have developed various vegetation indices based on the fact that plants reflect more in near infrared radiation but less in visible red light compared with non-vegetated surfaces (Li and Weng, 2005). Despite their limitations, vegetation indices such as NDVI and EVI are highly useful measurements for vegetation identification (Carlson and Ripley, 1997). NDVI was used in this study for urban classification.

(3) Texture images

Lu and Weng (2007) believed that the most significant variables for remote sensing image classification were spectral information. However, texture and context information should never be ignored, especially when high resolution remote sensing images are used. Texture measures such as Gray Level Co-occurrence Matrix (GLCM), spatial statistic based, signal analysis etc have already been developed and applied in remote sensing image classification. Some researchers determined that the most useful features for analyzing the content of remote sensing imagery were those variables calculated from using a GLCM approach (Shanmugan *et al.*, 1981; Pacifici *et al.*, 2009). So, three texture features derived from the GLCM have been considered in this work, namely Homogeneity, Dissimilarity and Entropy. Homogeneity measures the composition of similar images while Entropy indicates the disorder or heterogeneity in an image. Dissimilarity measures the difference in elements of the co-occurrence matrix from each other. Their formulation is shown in the following:

$$\text{Homogeneity} = \sum_{i=1}^{N-1} \sum_{j=1}^{N-1} \frac{p(i, j)}{1 + (i - j)^2}$$

$$\text{Dissimilarity} = \sum_{i=1}^{N-1} \sum_{j=1}^{N-1} p(i, j) \cdot |i - j|$$

$$\text{Entropy} = - \sum_{i=1}^{N-1} \sum_{j=1}^{N-1} p(i, j) \cdot \log(p(i, j))$$

where i and j are the gray tones in the windows or

the coordinates of the co-occurrence matrix space; $p(i, j)$ indicates the normalized frequencies with which two neighboring resolution cells separated by a fixed shift occur on the image (one with gray tone i and the other with gray tone j); N represents the dimension of the co-occurrence matrix.

In Earth sciences, many properties exhibit spatial clustering of similar values around an individual location. The local patterns of spatial association or spatial autocorrelation can be identified by local indicators of spatial association (LISA) measures. Local Moran's I and Getis-Ord Local G were two indices of spatial autocorrelation and they were computed for the three spectral bands as additional textural information in our classification. They are defined as (Han *et al.*, 2012)

$$\text{Local Moran's I}_i(d) = (x_i - \bar{x}) \sum_{j=1}^n w_{ij}(d) (x_j - \bar{x})$$

$$\text{Local Getis G}_i(d) = \frac{\sum_{j \neq i} w_{ij}(d) x_j}{\sum_{j \neq i} x_j}$$

where x_i and x_j are the values of variable x in i and j positions respectively; the mean of variable x is \bar{x} ; $w_{ij}(d)$ is the weight matrix between position i and j within distance d ; and n is the sample size;

A positive value for Local Moran's I indicates that the feature is surrounded by features with similar values. Such a feature is part of a cluster. A negative value for it indicates that the feature is surrounded by features with dissimilar values. Such a feature is an outlier. Getis-Ord Local G is useful for determining clusters of similar values where clusters of high values result in a high G_i value and clusters of low values result in a low G_i value (Shahtahmassebi *et al.*, 2014).

As for the window size, Shaban and Dikshit (2001) concluded that high resolution images usually need smaller window sizes than coarse resolution images. Considering the 10 meter spatial resolution of our image, all three bands with window sizes of 3×3 , 5×5 , 7×7 , 9×9 were calculated. Lag distance from 1 to 9 was also calculated by using Rook's Case.

(4) Shape related features

The urban area is a really complicated entity composed of many different types of constructions and natural objects. Different targets may share the same reflectance but have distinct shapes, for exam-

ple: a building and road. Concerning its nature in external appearance, we chose Area, Shape index and Length/width as three variables for participating in an Object based classification. Detailed descriptions of the three indexes can be found in the Reference Book of eCognition Developer 8.7.1 (Documentation, 2012).

(5) Feature selection

Wu *et al.* (2012) pointed out that classification accuracy could be significantly decreased when all possible features were used in a classification procedure. Feature selection seems to be inevitable. Forward stepwise linear discriminant analysis (LDA) was applied for assessing usefulness and the influences of the proposed descriptive features for our classification problem. In this method, the determination of the features which contribute most to land cover classification is realized by reviewing and evaluating all variables at each step. The model then includes that variable and processes the iteration (Hermosilla *et al.*, 2012).

(6) Variable importance measure

For better understanding the contribution of each variable in classification, a random forest algorithm was adopted. The random forest machine learner is a meta-learner; meaning it consists of many individual learners (trees). The random forest uses multiple random tree classifications to vote on an overall classification for the given set of inputs (Livingston, 2005). It provides a ranking of variable relevance by comparing classification accuracies obtained with, and then without, each of the features (Novack *et al.*, 2011). The reader is referred to Livingston (2005) for a detailed description of this algorithm.

2.5 Classification

Object oriented classification is usually deemed to be superior to a per-pixel classification approach because image objects can represent meaningful information while single pixels cannot (Mathieu *et al.*, 2007). Therefore, better classification results can be acquired, especially for fine spatial resolution data. We used an eCognition Developer 8.7 to perform an object-based classification approach. With this software, appropriate values need to be assigned to the three key parameters, namely shape, compactness, and scale in the object-based paradigm. The most

crucial parameter of image segmentation is the scale parameter that controls object size. By modifying the shape criterion, the color criteria can be indirectly defined (color=1-shape) to change the relative weighting of the reflectance and shape in defining the segments. The shape criterion is composed of two parameters: compactness and smoothness. The smoothness criterion is used to optimize image objects with regard to smoothness of borders while the compactness criterion is used to optimize image objects with regard to compactness. For the sake of paying more attention to spectrally homogeneous pixels for image segmentation, we set the shape parameter to be 0.1 to give less weight to the shape. Objects were balanced equally by setting compactness and smoothness parameters to be 0.5. Based on a trial-and-error analysis, we found that a scale parameter of 5 was appropriate for this study. After segmentation, a support vector machine (linear kernel) algorithm was applied for classification of the whole image. It is important to mention that the image was firstly classified into 26 classes according to the reflectance of each land cover, then all classes were merged into 7 classes with reference to our classification system. The system was built based on a U.S Geological Survey Land-use/Land-cover classification system for use with remote sensor data modified for the national land cover dataset and a NOAA coastal change analysis program (NOAA, 2004). According to the specific situation of Hangzhou city, some revisions have been done to make it more suitable for a China study. Our classification system was composed of 7 classes: Residential, Commercial/Industrial/Transportation, Forest, Groves, Water, Barren and Farmland.

2.6 Accuracy assessment

To perform the object-based accuracy assessment, a total of 760 (no less than 50 for each class) land-cover polygons or objects were randomly selected from the study site in Hangzhou city. The polygons were visually interpreted with reference to the land-use map and field survey data and compared with the classification results derived from the object-based approach. It is important to mention that the 26 original classes were grouped into 7 classes before computing the accuracy indexes as explained

later.

The comparison between predicted classes derived from the classifier and visual interpreted classes with reference to the land use map was realized by means of error matrices. Several indexes such as Producer's accuracy (PA), User's accuracy (UA), Overall accuracy (OA) and Kappa indexes were calculated from this matrix. UA implies commission errors (i.e. when an object is committed to an incorrect class), while PA details omission errors (i.e. when a segment is incorrectly classified into another category and so it is omitted from its correct class). Furthermore, OA is the ratio of the number of correctly classified objects to the total number of objects. Finally, the off-diagonal observations of the rows and columns and diagonal values of the error matrix are incorporated by the kappa statistic index so that a more robust accuracy assessment can be given by this index than through OA measures (Aguilar *et al.*, 2013).

Besides the points based accuracy assessment, an area residual approach is another aspect that can imply classification accuracy. Forty-five sample plots with 50×50 pixel sizes (i.e., $500 \text{ m} \times 500 \text{ m}$) were selected from the classified image. We selected plots from intersections between straight lines and cycles,

with a distance of 200 pixels between two cycles (Fig.3). Reference plots were acquired by visual interpretation of each square with reference to the land use map in which several classes were included. Finally, a comparison was conducted between classified plots and reference plots using the PAC index. A formula description of this index is shown as follows:

$$W_s = \frac{A_i}{B_i} \times 100\%$$

W_s : Polygon Area Consistency; A_i : common area between sample and reference; B_i : reference area.

3 Results and discussion

3.1 Feature analysis

For the GLCM and Spatial autocorrelation group, selected variables were (1) Homogeneity_R_3×3, Dissimilarity_G_9×9, Entropy_R_9×9; and (2) Moran_G_9, Moran_NIR_9, Getis_NIR_3 (first word means texture second character implies band, number represents window size). As is shown in Fig. 4, the window size 9×9 was suitable for Dissimilarity and

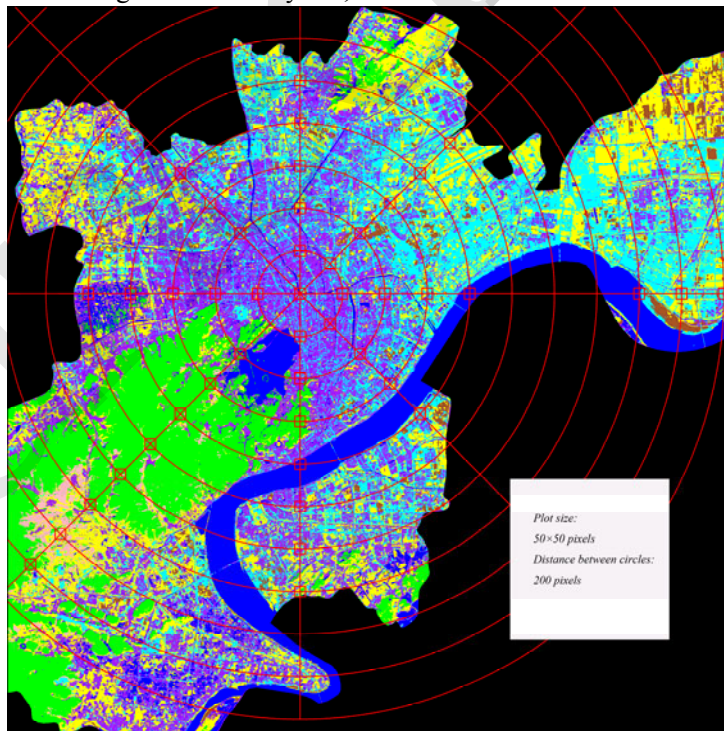


Fig. 3 Strategy for collection of reference data for the accuracy assessment of the area, illustrating the approach for allocating sample plots on the classified image

Entropy, but a window size 3×3 is needed for Homogeneity. It was found that a lag distance of 9 was optimal for Moran's I, but 3 is necessary for Getis Gi. Each multispectral band had its own advantages in the texture calculation. All variables selected by LDA displayed their contribution to accuracy improvement according to Fig. 4. It was clear that the classification accuracy increased steadily when GLCM, spatial autocorrelation and three shape indexes were gradually included. We can see from the first part of the Figure that there was a dramatic increment when three multispectral bands were progressively included. However, no obvious mounting can be found when the NDVI and fraction of impervious surface images were added in. This could be explained by the following reasons: (1) information contained in the NDVI and fraction images almost overlapped with the original bands or they were useless in their classification. (2) importance of the two variables were far below that of the three original bands so that the influence cannot be illustrated even if they made some tiny contribution. (3) they did have their function and that influence was really large, but it cannot be answered by linear projection no matter how many discriminant models were built. To understand the exact reasons, a correlation analysis of the first eleven variables were presented in the heat map (Fig. 5).

As can be seen from Fig. 5, there was a high correlation between the Green and Red bands, and the

correlation coefficient can be higher than 0.8. Correlation between the Red band and fraction image of the impervious surface (Imp) were similar to that of the multispectral bands. NDVI had little correlation with the near-infrared band or low correlation with most of the other variables. Therefore, we deemed that the information overlap was not a core problem even though correlation between the Red band and the impervious surface fraction reached a high level, not to disregard the low correlation between NDVI and the other variables. An assumption of information overlap can be excluded. In addition, spatial autocorrelation variables (Moran_NIR_9 and Moran_G_9) exhibited little correlation with almost all variables.

It was evident in Fig. 6 that the spatial autocorrelation measures were identified to be the most important variables, especially for Moran's I calculated from the Near-infrared band with a lag distance of 9. GLCM based variables not getting a high rank may be attributed to the relatively high correlation between these variables and the original spectral bands. NDVI and the impervious surface fraction were two variables that had almost the same significance with the original three bands according to this algorithm. This was easily understood because NDVI was originally designed for vegetation detection. Impervious surface fraction indicates the percentage of impervious surface in every pixel. Every land-use was normally

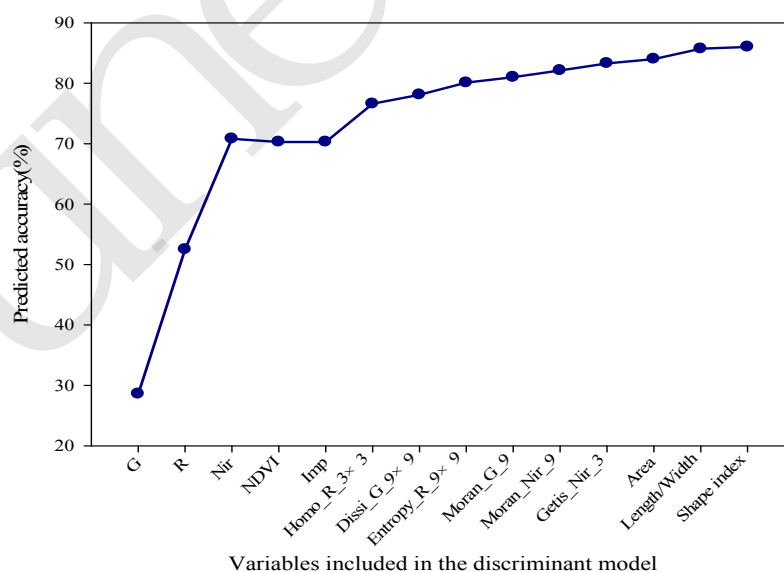


Fig. 4 Predicted cross-validated classification accuracy when the 14 features were progressively included in the discriminant model

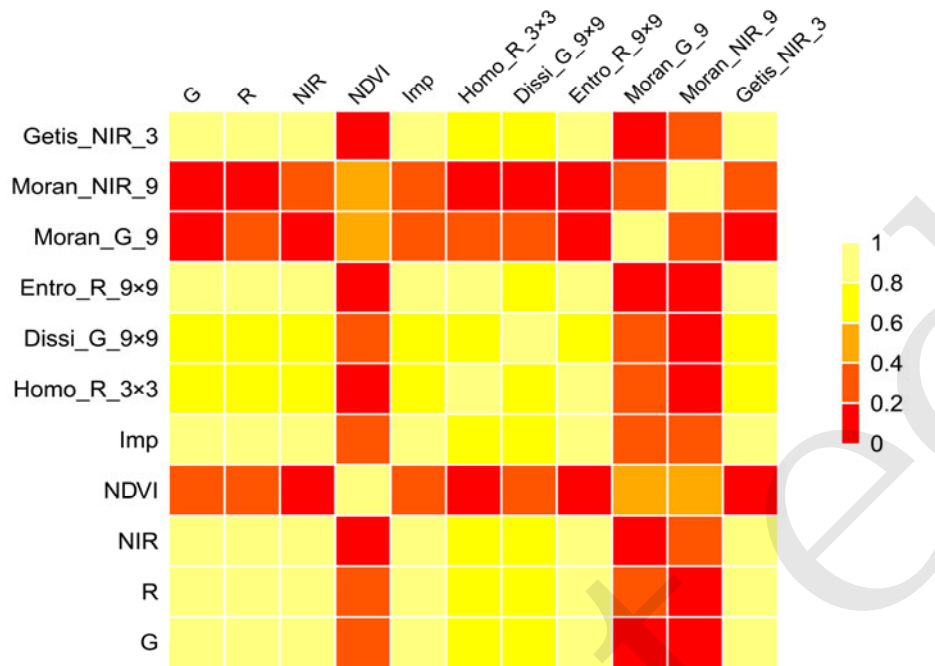


Fig. 5 Correlation of eleven variables indicated by correlation coefficient

characterized by its own impervious surface distribution. Normally, the impervious surface of the industrial section should be higher than that of the residential to gain profit as much as possible. As expected, the three shape related features appeared to be the least significant among the whole data set. The reason why spatial autocorrelation outperformed other variables could be explained by the fact that the city area was mostly covered by residential buildings which in fact were auto correlated in every block. Another possible reason would be that the land-use pattern in Hangzhou was highly policy oriented, in other words, every construction project should be consistent with land-use planning which was usually spatial auto correlated in a small area.

As mentioned above, NDVI and impervious surface fraction images were essential variables that had low correlation with the three original bands. Although a high correlation was found between the Green and Red band, none of them were abandoned because a small discrepancy may imply a huge power of discrimination for the land cover. Thus, all of the 14 variables (multispectral bands included) were applied in the subsequent object oriented classification.

3.2 Classification analysis

Feature analysis was based on statistics of samples which depended on accurate selection of the variables. Classification provided an approach for demonstrating the usefulness of that method. As was shown in Fig. 7 and Table 2, overall classification accuracy was satisfactory. Most classes were correctly classified owing to those selected important variables. However, as we had mentioned before, Hangzhou is a historical city undergoing a developing progress. Ancient architectures, modern commercial buildings, modern residential apartments, private houses as well as rural housing mixed together generated a great challenge. Second, since this image was captured on February 2012, a shadow casted by high buildings and mountains was also a factor that cannot be ignored. We merged shadow into residential buildings in this study which contributed to part of the errors. Moreover, water is widely spread throughout the southern part of the city with various forms like: rivers, lakes, ponds, paddy fields, etc. A big discrepancy could be found between different forms of water due to diversities of reflectance from the water's surface. Similarity of shadow, different forms of water and dark roof buildings was another factor causing erroneous classification.

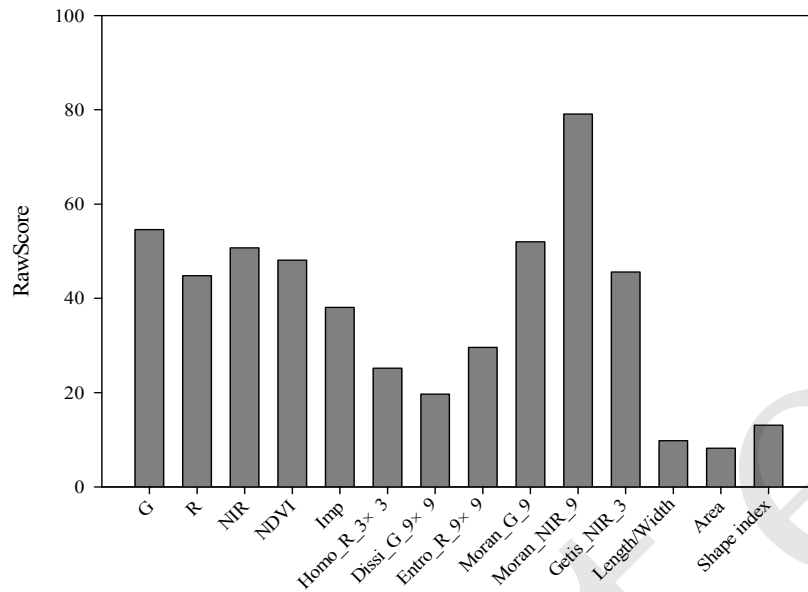


Fig. 6 Variable importance provided by random forest algorithm

Examining the error matrix (Table 2) derived from the object oriented classification approach, we found that water and groves had the highest user's accuracy while farmland had the highest producer's accuracy. This could be attributed to its characteristic of high value in NDVI. Next to the vegetation and water land-use, commercial/industrial/transportation producer's and user's accuracy were the second highest. This could be explained by the trait of high response in impervious surface fraction, area differences and autocorrelation distinction. Also, industrial, civic, and office land use usually tend to cluster, to gain the maximum benefit, a situation that is expected to occur more in the future. In contrast to office and industrial land use, civic land use belongs to non-profit land use (Hu and Wang, 2013). Here the barren producer's and user's accuracy were the lowest. We can see from Table 2 that the barren data was mostly confused with residential and commercial/industrial/transportation. The reason can be found in Fig. 7 where the densely distributed residential buildings were easily misclassified into barren for their resemblance in both texture and reflectance. Roads located in industrial areas resulted in another error of barren misclassification. Some confusion also existed between residential and commercial/industrial/transportation. The low user's accuracy of

the residential class is indicated by the misclassification of commercial/industrial/transportation into residential. This problem occurs between narrow roads with low DN number and dark roof residential buildings.

The error matrix shows that farmland parcels had a high degree of confusion with residential, and forests. As shown in Fig. 7, this problem emerged in the northern mountain area in which human planted trees and natural ones grow together forming its own texture. Other possible reasons for the low accuracy of farmland could be due to the error of the land use map or land cover change from the fall of 2010 to the spring of 2012. A proper method that may solve this problem is to use topographic data. Forests usually show their appearance on mountains while farmland normally occurs on the planes. Moreover, Hangzhou is a tourist city so that the vegetation coverage is a significant factor for government decision-making. Some residential blocks featured such a high level of vegetation coverage that they were reckoned as farmland by the classifier.

Table 2 Overall accuracy, producer's accuracy, user's accuracy, and kappa coefficient produced by object-oriented classifier

Classified Data	Reference								PA(%)	UA(%)
	Residential	Commercial/Industrial/Transportation	Forest	Groves	Water	Barren	Farmland	Totals		
Residential	153	7	2	0	5	2	2	171	94.44	89.47
Commercial/Industrial/Transportation	1	131	0	0	2	3	2	139	90.34	94.24
Forest	0	0	110	3	1	0	1	115	94.02	95.65
Groves	0	0	0	56	0	0	0	56	91.80	100.00
Water	0	0	0	0	91	0	0	91	91.92	100.00
Barren	3	3	0	0	0	55	0	61	87.30	90.16
Farmland	5	4	5	2	0	3	108	127	95.58	85.04
Total	162	145	117	61	99	63	113	760		

Overall Classification Accuracy = 92.63%

Overall Kappa Statistics = 0.9124

Water was a third major error (omission error represented by relatively low producer's accuracy) in the classification. In other areas, water could not be a problem. However, as we had discussed before, Hangzhou was a typical southern city covered with various kinds of water including river, lake, pond and wetland. The reason that may explain the confusion between water and residential could be summarized as follows: (1) From Fig. 7, south Hangzhou was primarily covered by ponds. The DN value, as well as

the shape index of the dark residential, to a large extent, resemble that of ponds. (2) Rivers usually develop their own branches, and some of these branches were so narrow that could not be segmented even with a very small scale parameter. Average reflectance of these objects looked like those of dark residential segments. (3) The shadow, whose reflectance was similar to water in an urban area, was merged into residential, which interferes with accuracy.

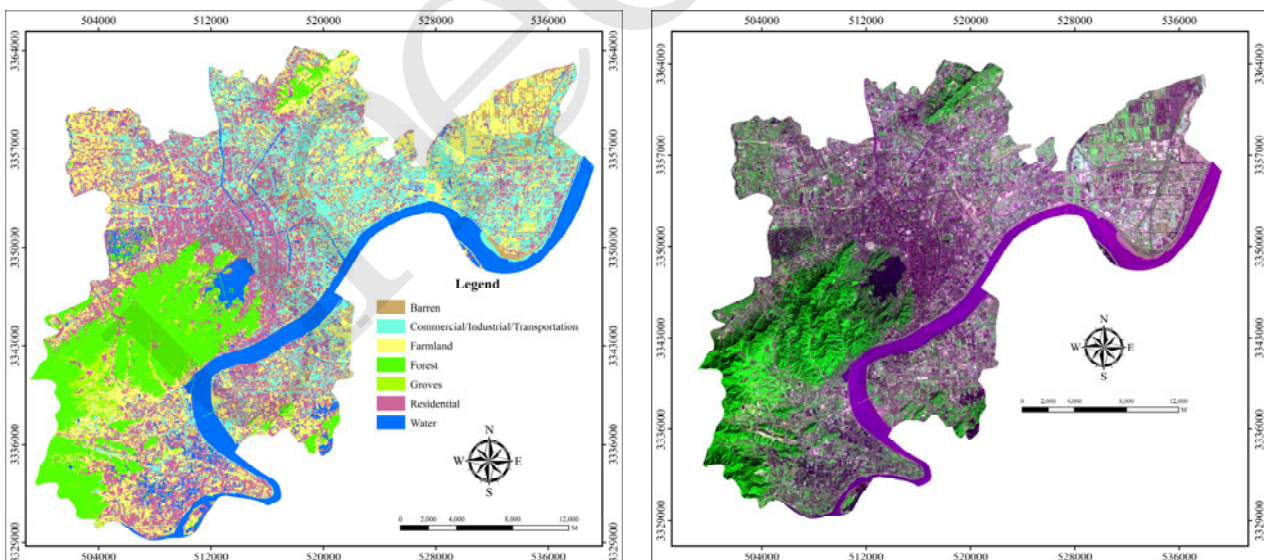


Fig. 7 Original image (R:2,G:3,B:1) and land use/cover map of Hanhzhou city produced by object oriented classification

3.3 Area analysis

Identification of forest achieved the highest accuracy according to the area evaluation index (Fig. 8). This was in agreement with the point based accuracy assessment indicating the robustness of the forest detection, using the proposed method. According to the PAC index, farmland attained the second highest accuracy. This was the opposite with its low user's accuracy in the error matrix. A probable reason could be that this class was overestimated in the final classification. Overestimation of this class resulted in a larger common area which improved the performance of this index and reduced the classification accuracy that could be illustrated by a point based accuracy assessment. Residential and water were two classes that displayed the lowest accuracy due to their really complicated forms of distribution as well as the

shortage of blue band, because many researchers believed that the NDBI (normalized difference of built up index) was useful for built up area extraction in which the blue band was included. Barren was not a widely distributed class, the area evaluation index of this class was easily suffered by its small total sample area. Therefore, its final accuracy was prone to be affected by several large segments. Future work could collect more barren samples for area analysis. The superiority of the sampling scheme adopted by our study was reflected in its randomness and representativeness of all 8 directions.

Overall, the area evaluation result was satisfactory though the accuracy of a very few classes were not high enough, area precision of most classes exceeded 82%, which we deemed was acceptable for most applications.

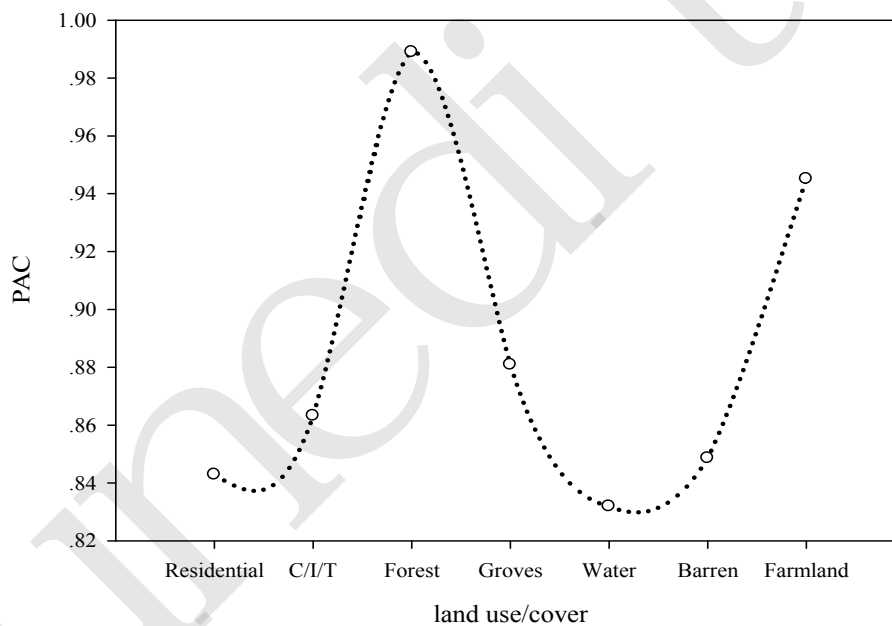


Fig. 8 Area evaluation result.(C/I/T represent commercial/industrial/transportation)

4 Conclusions

This research is, to our knowledge, one of the few investigations of urban landscape classification using China's satellite ZY-1 02C multispectral image in Hangzhou city. Although this satellite has only three bands, a relatively satisfactory result is obtained using an object-oriented approach with the combination of various categories of variables selected by the

LDA. Variable importance analysis illustrated that the spatial autocorrelation was of the most significance during the classification, which could be attributed to land-use planning and construction characteristics of this city. Shortcomings of this research include barren, farmland and residential misclassification that need to be overcome through further data mining techniques.

Note that this study focuses mainly on exploring the feasibility of integration of different categories of

variables in obtaining an acceptable classification result by means of the Chinese 02C imagery. Thus, a random forest was used instead of comparing different classification results with disparate variables. Area analysis with a PAC index proved that an acceptable area accuracy could be attained, meanwhile, overestimation of farmland and the relatively low accuracy of residential or water need to be solved by other approaches. Statistical analysis with various combinations of variables and their role in land cover recognition is left to our future work.

In conclusion, we proposed a method that integrated five categories of variables using the combination of LDA and the random forest algorithm. Results derived from this method illustrated its effectiveness for urban landscape classification. It also revealed the high quality of the Chinese ZY-1 02C multispectral image. Variable importance extracted from GLCM, spatial autocorrelation, and a shape related index proved the data's reliability for texture calculations. Future work can focus on inclusion of other variables for detailed classification or for comparison of the accuracy of the classification between this data and that of other similar spatial/spectral resolution data such as SPOT.

Reference

- Adams, J.B., Sabol, D.E., Kapos, V., et al., 1995. Classification of multispectral images based on fractions of endmembers: Application to land-cover change in the Brazilian Amazon. *Remote Sensing of Environment*, **52**(2): 137-154. [doi: 10.1016/0034-4257(94)00098-8].
- Aguilar, M.A., Saldaña, M.M., Aguilar, F.J., 2013. GeoEye-1 and WorldView-2 pan-sharpened imagery for object-based classification in urban environments. *International Journal of Remote Sensing*, **34**(7): 2583-2606. [doi: 10.1080/01431161.2012.747018].
- Carlson, T.N., Ripley, D.A., 1997. On the relation between NDVI, fractional vegetation cover, and leaf area index. *Remote Sensing of Environment*, **62**(3): 241-252. [doi: 10.1016/S0034-4257(97)00104-1].
- Chen, Y., Shi, P., Fung, T., et al., 2007. Object - oriented classification for urban land cover mapping with ASTER imagery. *International Journal of Remote Sensing*, **28**(20): 4645-4651. [doi: 10.1080/01431160500444731].
- Deng, J.S., Wang, K., Deng, Y.H., et al., 2008. PCA-based land - use change detection and analysis using multitemporal and multisensor satellite data. *International Journal of Remote Sensing*, **29**(16): 4823-4838. [doi: 10.1080/01431160801950162].
- Documentation, T., 2012. eCognition Developer 8.7. 1: Reference Book. Trimble Germany GmbH, Munich, Germany.
- Durieux, L., Lagabrielle, E., Nelson, A., 2008. A method for monitoring building construction in urban sprawl areas using object-based analysis of Spot 5 images and existing GIS data. *ISPRS Journal of Photogrammetry and Remote Sensing*, **63**(4): 399-408. [doi: 10.1016/j.isprsjprs.2008.01.005].
- Han, N., Wang, K., Yu, L., et al., 2012. Integration of texture and landscape features into object-based classification for delineating Torreya using IKONOS imagery. *International Journal of Remote Sensing*, **33**(7): 2003-2033. [doi: 10.1080/01431161.2011.605084].
- Hermosilla, T., Ruiz, L.A., Recio, J.A., et al., 2012. Assessing contextual descriptive features for plot-based classification of urban areas. *Landscape and Urban Planning*, **106**(1): 124-137. [doi: 10.1016/j.landurbplan.2012.02.008].
- Hu, S., Wang, L., 2013. Automated urban land-use classification with remote sensing. *International Journal of Remote Sensing*, **34**(3): 790-803. [doi: 10.1080/01431161.2012.714510].
- Jacquin, A., Misakova, L., Gay, M., 2008. A hybrid object-based classification approach for mapping urban sprawl in periurban environment. *Landscape and Urban Planning*, **84**(2): 152-165. [doi: 10.1016/j.landurbplan.2007.07.006].
- Li, G., Weng, Q., 2005. Using Landsat ETM+ imagery to measure population density in Indianapolis, Indiana, USA. *Photogrammetric engineering and remote sensing*, **71**(8): 947.
- Livingston, F., 2005. Implementation of Breiman's random forest machine learning algorithm. *ECE591Q Machine Learning Journal Paper*.
- Lu, D., Weng, Q., 2006. Use of impervious surface in urban land-use classification. *Remote Sensing of Environment*, **102**(1): 146-160. [doi: 10.1016/j.rse.2006.02.010].
- Lu, D., Weng, Q., 2007. A survey of image classification methods and techniques for improving classification performance. *International journal of Remote sensing*, **28**(5): 823-870. [doi: 10.1080/01431160600746456].
- Mathieu, R., Freeman, C., Aryal, J., 2007. Mapping private gardens in urban areas using object-oriented techniques and very high-resolution satellite imagery. *Landscape and Urban Planning*, **81**(3): 179-192. [doi: 10.1016/j.landurbplan.2006.11.009].
- Novack, T., Esch, T., Kux, H., et al., 2011. Machine learning comparison between WorldView-2 and QuickBird-2-simulated imagery regarding object-based urban land cover classification. *Remote Sensing*, **3**(10): 2263-2282. [doi: 10.3390/rs3102263].
- Pacifici, F., Chini, M., Emery, W.J., 2009. A neural network approach using multi-scale textural metrics from very high-resolution panchromatic imagery for urban land-use classification. *Remote Sensing of Environment*, **113**(6): 1276-1292. [doi: 10.1016/j.rse.2009.02.014].

- Ridd, M.K., 1995. Exploring a VIS (vegetation-impervious surface-soil) model for urban ecosystem analysis through remote sensing: comparative anatomy for cities†. *International Journal of Remote Sensing*, **16**(12): 2165-2185. [doi: 10.1080/01431169508954549].
- Settle, J.J., Drake, N.A., 1993. Linear mixing and the estimation of ground cover proportions. *International Journal of Remote Sensing*, **14**(6): 1159-1177. [doi: 10.1080/01431169308904402].
- Shaban, M.A., Dikshit, O., 2001. Improvement of classification in urban areas by the use of textural features: the case study of Lucknow city, Uttar Pradesh. *International Journal of Remote Sensing*, **22**(4): 565-593. [doi: 10.1080/01431160050505865].
- Shahtahmassebi, A., Pan, Y., Lin, L., et al., 2014. Implications of land use policy on impervious surface cover change in Cixi County, Zhejiang Province, China. *Cities*, **39**: 21-36. [doi: 10.1016/j.cities.2014.02.002].
- Shanmugan, K.S., Narayanan, V., Frost, V.S., et al., 1981. Textural features for radar image analysis. *IEEE Transactions on Geoscience and Remote Sensing*, (3): 153-156. [doi: 10.1109/TGRS.1981.350344].
- Smith, M.O., Ustin, S.L., Adams, J.B., et al., 1990. Vegetation in deserts: I. A regional measure of abundance from multispectral images. *Remote sensing of Environment*, **31**(1): 1-26. [doi: 10.1016/0034-4257(90)90074-V].
- Wu, B., Wang, X., Shen, H., et al., 2012. Feature selection based on max-min-associated indices for classification of remotely sensed imagery. *International Journal of Remote Sensing*, **33**(17): 5492-5512. [doi: 10.1080/01431161.2012.663111].